RESEARCHERID
THOMSON REUTERS

[Nakamura* 8(3): March, 2021] ISSN 2349-4506
Impact Factor: 3.799

Global Journal of Engineering Science and Research Management

EFFECT OF ASH CONTENT ON STEAM GASIFICATION OF HEAVY OIL FLY ASH

Ayano Nakamura[*1], Taishi Nakajima[2] & Kenji Murakami[3]
[*1,2&3]Department of Materials Science, Faculty of Engineering Science, Akita University, Akita City, Japan

DOI: 10.5281/zenodo.4660039

KEYWORDS: Heavy oil fly ash, Steam gasification, Catalyst, Flammable gas.

ABSTRACT

The heavy oil fly ash (HOFA) generated from the oil-thermal power plants is usually disposed by landfill. However, HOFA contains a large amount of unburned carbon and heavy metal components, so that HOFA disposed as industrial waste was more costly than general waste. The steam gasification, which is expected to generate flammable gas, has attracted attention as an effective method of utilizing HOFA. When the steam gasification of HOFA at 700-800ºC was performed, H_2, CO and CO_2 were produced, and the amount of H_2 evolution was the largest among these evolution gases. Furthermore, the amount of H_2 evolution increased with increasing ash content in HOFA. In particular, the amount of H_2 evolution with HOFA of 20 wt% ash contents was 179 mmol/g-char at 800ºC for 60 min. From XRD pattern of HOFA, iron oxide and nickel oxide were reduced before steam gasification. The amount of H_2 evolution increased with increasing Fe and Ni contents in HOFA, suggesting that Fe and Ni species act as catalysts.

INTRODUCTION

The ratio of thermal power plants in Japan accounts for about 80% of the total electric energy, and fossil fuels such as coal, petroleum (heavy oil), and natural gas are mainly used for power generation. Fly ash is generated by burning the coal and petroleum and collected in filter bags. In particular, the amount of heavy oil fly ash (HOFA) generation exceeds 100 tons in a month at a 350,000 kW oil-fired power plant [1], and these HOFA generated are usually landfilled. Since HOFA, which contains heavy metal components, was discarded as industrial waste, a landfill place for HOFA was required [1]. However, the industrial waste disposal is more costly than general waste one, so that it is necessary to utilize effectively or reuse HOFA. In previous studies, one of the effective utilization is to recovery heavy metal components such as Ni and V from HOFA [2-4]. However, many extraction / separation steps are required to separate heavy metal components. Also, in order to investigate whether HOFA containing a large amount of unburned carbon is able to use as fuel, some researches have already been conducted regarding to combustion behavior of HOFA alone or mixtures of HOFA with waste plastic and sewage sludge [1,5,6]. The combustibility of HOFA, which is low (calorific value 25-30 kJ/g, activation energy:160-185 kJ/mol), was not significantly improved even when mixed with combustible plastic or sludge.

It was considered that flammable gas (H_2, CO) can be obtained by steam gasification at low temperature using HOFA containing a large amount of unburned carbon and heavy metal components. Heavy metals such as Fe and Ni, alkali metals such as Na and K, and alkaline earth metals such as Ca, are known to be highly effective as catalysts for steam gasification [7-10]. Yang et al. [11] are investigating the gas evolution behavior with iron ore added as a catalyst to bituminous coal. When the mixture ratio of iron ore and the gasification temperature (600-1000 ºC) are changed, it is reported that the amount of H_2 and CO evolution increased with increasing the iron ore / coal ratio at 800ºC. A previous study of authors [12] also found that impregnation to Adaro subbituminous coal with $FeCl_2$ increased the amount of H_2 evolution.

As a matter of fact, since many heavy metal components, such as iron oxide and nickel oxide, are present in HOFA, these components are expected to act as catalysts for enhancement of steam gasification at a lower temperature. However, there have been no research reports on steam gasification of HOFA. In this study, the steam gasification of HOFA with different heavy metal contents is performed, and the effect of heavy metal components and quantity in HOFA on the amount of gas evolution is investigated.

EXPERIMENTAL

Materials

HOFA with a particle size of 1-200 μm was provided by the Akita Thermal Power Station of Tohoku Electric Power Co., Inc. HOFA samples were used after drying at 110 ºC for 2 days. The ash content was measured by following the procedure with reference to JIS M 8812 [13]. The dried HOFA 1 g was added in an alumina sintered dish (30 x 50 x 10 mm), heated to 815 ºC for 60 min using an electric furnace (SHIROTA SUPER100T), and maintained at the same temperature for 2 h. After heating, it was cooled for 10 min on a stainless steel plate and for 15 min in a desiccator, and the sample after cooling was defined as ash. Also, the dried HOFA 1g was heated at 900 ºC for 7 min into a platinum crucible. After that, it was cooled by the same method as above, and the weight loss of the sample was taken as the volatile matter. The fixed carbon was obtained by subtracting the ash and volatile matter from 100 wt%. Table 1 shows the proximate analysis and ultimate analysis of various HOFA, and the ash content in HOFA is HOFA-1 < HOFA-2 < HOFA-3.

Table 1. Proximate and ultimate analysis of HOFA

	Proximate analysis wt% (dry)			Ultimate analysis wt% (daf)			
Sample	Ash	V.M.	F.C.	C	H	N	O
HOFA-1	10.6	17.4	72.0	72.1	0.8	3.5	23.6
HOFA-2	15.8	17.2	67.1	75.0	0.7	2.2	22.1
HOFA-3	20.1	40.5	39.4	50.0	1.5	5.5	43.0

Table 2 shows the ash composition in HOFA obtained by X-ray fluorescence (XRF) analysis (Shimadzu, XRF-1700 4kW). For XRF analysis, the ash obtained by burning HOFA at 900 ºC for 2 h was pelletized at a pressure of 28 tons. And, the ash composition of HOFA shown in Table 2 were calculated by multiplying the ratio of ash content.

Table 2. Ash composition of HOFA by XRF [wt.%, dry]

Metal oxide	HOFA-1	HOFA-2	HOFA-3
Fe_2O_3	1.19	4.23	10.8
SiO_2	2.52	2.69	1.40
Al_2O_3	1.96	2.29	1.17
SO_3	1.24	1.78	1.85
NiO	1.31	1.58	1.82
Na_2O	0.57	1.06	0.93
CaO	0.76	0.82	0.64
V_2O_5	0.39	0.41	0.51
K_2O	0.11	0.24	0.22
MgO	0.14	0.19	0.17
Co_2O_3	0.09	0.10	0.13
P_2O_5	0.10	0.09	0.09
TiO_2	0.06	0.07	0.06
ZnO	0.04	0.06	0.13
BaO	0.04	0.05	0.07
La_2O_3	0.07	0.05	0.01
MnO	0.02	0.03	0.06
CuO	0.01	0.02	0.03
SrO	0.01	0.01	0.01
Total	10.63	15.77	20.10

Demineralization of HOFA

HOFA was demineralized in order to investigate the effect of ash in HOFA on gasification. HOFA (10 g) was added to 12 M of hydrochloric acid (150 mL) in a beaker, and HOFA suspension was stirred using a hot stirrer at

450 rpm and 30 ºC for 24 h. Afterward, the suspension was washed with distilled water until the filtrate became neutral during suction filtration, and the filtration residue was dried at 110 ºC for one day. The metal morphology in demineralized HOFA (DHOFA) was evaluated by X-ray diffraction (XRD) analysis (Rigaku, Ultima IV). The measurement conditions for XRD analysis were set to a scanning from 10º to 80º at intervals of 0.02º, and a scanning rate of 10º/min, and the measurement were performed using CuKα radiation at 40 kV and 40 mA.

Pyrolysis and steam gasification

Pyrolysis and steam gasification were performed using the fixed bed reactor shown in Fig.1. Quartz wool of 0.2 g and HOFA of 0.5 g were inserted into a quartz reaction tube (ϕ17 mm). At this time, the height of HOFA layer was 9 mm. Argon (Ar) gas as a carrier was flowed at 140 mL/min for 30 min to purge air in the reaction tube.

The HOFA was heated to 700, 750, and 800ºC using a ceramic tube furnace (Asahi-rika, ARF-40K). After heating up to the predetermined temperature, HOFA was pyrolyzed for 10 min while flowing Ar gas and HOFA char was obtained. After pyrolysis for 10 min, Ar gas was flowed to the steam generator set at 87ºC, and the steam gasification was carried out for 60 min while flowing 60 vol% of steam in HOFA layer. After steam gasification, the steam flow was switched to Ar flow for 10 min at the same temperature. Then, the sample was cooled to room temperature. The gaseous component generated during steam gasification was collected by V_0 = 0.5 mL every 6 min and analyzed by on-line gas chromatograph (GC) (Shimadzu, GC2014), and the gas flow rate was measured by a soap-film flow meter (HORIBA STEC, VP-3U). HOFA samples after pyrolysis and steam gasification were analyzed by XRD under the same conditions as in section 2.2.

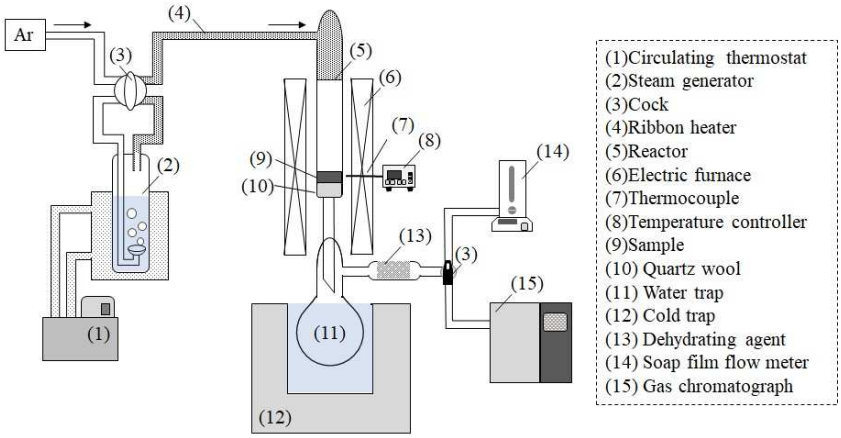

Fig. 1. Fixed-bed reactor for pyrolysis and steam gasification

In addition, the sample weight after pyrolysis was measured, and the yield of HOFA char (Y_{Char} [wt%]) based on dry and ash free was calculated with Eq. (1).

$$Y_{\mathrm{Char}} = \frac{W_{\mathrm{Char}} - (W_{\mathrm{s}} \times X_{\mathrm{Ash}})}{W_{\mathrm{s}} - (W_{\mathrm{s}} \times X_{\mathrm{Ash}})} \times 100 \quad (1)$$

Where W_{Char} is the weight of char after pyrolysis [g], W_{s} is the weight of HOFA sample before pyrolysis [g], and X_{Ash} is the ratio of ash [-]. Furthermore, as shown in Eq. (2), the carbon content in evolution gas by steam gasification is divided by the carbon content present in the char before steam gasification, and the carbon conversion, X_{Carbon} [mol%], is obtained as follows:

$$X_{\mathrm{Carbon}} = \frac{C_{\mathrm{Gas}}}{C_{\mathrm{Char}}} \quad (2)$$

$$C_{\mathrm{Char}} = \frac{W_{\mathrm{Char}} - (W_{\mathrm{s}} \times X_{\mathrm{Ash}})}{A_{\mathrm{w}}} \quad (3)$$

where C_{Gas} is the molar content of carbon amount in evolution gases such as CO and CO_2 [mol], and C_{Char} is the molar content of carbon originally contained in the HOFA char [mol], A_{w} is atomic weight of carbon [g/mol]. In

this study, it is assumed that the residue obtained by subtracting the ash content from W_{Char} is composed of only carbon. The specific rate was calculated to investigate the change in carbon conversion against the residual carbon in HOFA char, and is defined as follows:

$$R_{Sp} = \frac{R_{Carbon}}{W_{RChar}} \quad (4)$$

where R_{Carbon} is the carbon conversion rate [mol%/h], and W_{RChar} is the amount of residual carbon in HOFA char [mol%]. Arrhenius plot shown in Fig.2 can be obtained by plotting R_{Sp} at the carbon conversion of 5 mol% against the reciprocal of temperature. The activation energy during the steam gasification reaction was calculated from Eq. (5) from the slope of the straight line as follows:

$$R_{Sp} = A\exp\left(-\frac{E_a}{RT}\right) \quad (5)$$

where A is the frequency factor [1/s], E_a is the activation energy [kJ/mol], R is the gas constant [kJ/(mol·K)] and T is the absolute temperature [K].

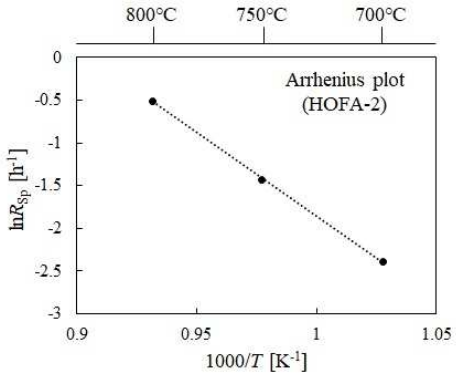

Fig. 2. Arrhenius plot with HOFA-2

RESULTS AND DISCUSSION

Chemical from of HOFA before and after pyrolysis

Fig.3 shows the XRD patterns of HOFA and HOFA char after pyrolysis at 800ºC. Iron oxide (Fe_3O_4) peaks were observed in all HOFA samples before pyrolysis, while the peak intensity of Fe_3O_4 decreased and the peaks attributed to α-Fe and Fe_3C appeared after pyrolysis at 800ºC. Also, nickel oxide was not detected in the XRD pattern before pyrolysis, but peaks attributed to Ni appeared after pyrolysis at 800ºC. This is because nickel oxide before pyrolysis is finely dispersed in HOFA. These results indicate that iron oxide and nickel oxide in HOFA were reduced during pyrolysis. Here, the ash contents shown in Table 1 are recalculated assuming that iron oxide and nickel oxide have been reduced in the pyrolyzed HOFA char, and the results are shown in Table 3.

Table 4 shows the char yield calculated using the ash content after pyrolysis in Table 3. From Table 4, the char yield after pyrolysis decreased for all HOFA samples, and HOFA-3 char especially decreased down to about 50 wt%. Also, the char yield tends to decrease slightly with increasing pyrolysis temperature. As shown in Fig.3 of XRD patterns, it was found that not only the metal oxide was reduced, but also the peaks of ammonium sulfate disappeared, indicating that a part of decreasing in char weight is due to the thermal decomposition of the ammonium sulfate contained in the HOFA.

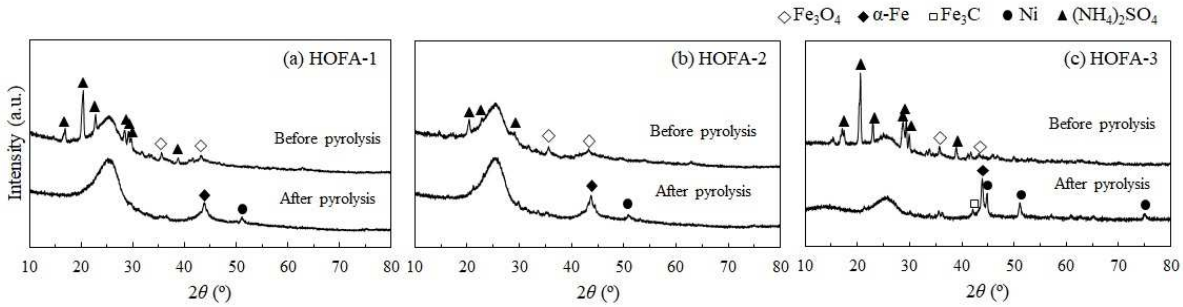

Fig. 3. XRD patterns for (a) HOFA-1, (b) HOFA-2 and (c) HOFA-3 before and after pyrolysis

Table 3. Fly ash ratio in HOFA before and after pyrolysis [%, dry]

Sample	Before pyrolysis	After pyrolysis
HOFA-1	10.6	10.0
HOFA-2	15.8	14.2
HOFA-3	20.1	16.5

Table 4. Char yield for HOFA after pyrolysis at different temperature [%, daf]

Sample	700°C	750°C	800°C
HOFA-1	78	78	77
HOFA-2	83	81	80
HOFA-3	55	50	49

Evolution gases and carbon conversion by steam gasification

The gas evolution rate at different temperature of steam gasification was shown in Fig.4. Also, Fig.5 shows the relationship between the steam gasification temperature and the carbon conversion. The steam gasification of HOFA produced H_2, CO and CO_2. Additionally, as the gasification temperature increased, all gas evolution rates and the carbon conversion increased regardless of the type of HOFA.

Table 5 shows the amount of evolution gas per 1 g of HOFA char and the carbon conversion. As shown in Table 5, there was a tendency for the amount of H_2 evolution to increase with increasing the carbon conversion. Using HOFA-1, the amount of H_2 evolution was the largest among the evolution gases, and the amount of CO evolution was as large as the amount of CO_2 evolution. In the case of HOFA-2 and HOFA-3, the amount of evolution gas increased in the order of $CO < CO_2 < H_2$. On the other hand, when the ash content in HOFA increased, the amount of CO evolution decreased and the amounts of H_2 and CO_2 evolution increased, suggesting that the ash content in HOFA affects the evolution of these gases. In addition, the amount of evolution gases after 60 min of steam gasification for all HOFA samples had the relationship as shown in Eq. (6).

$$(\text{Amount of } H_2 \text{ [mol]}) = (\text{Amount of CO [mol]}) + (\text{Amount of } CO_2 \text{ [mol]}) \times 2 \qquad (6)$$

This relationship was also seen when the steam gasification of Adaro subbituminous coal was carried out [9,12]. The main reactions in steam gasification are shown as follows [14-16].

$$C + H_2O \leftrightarrow H_2 + CO \qquad (7)$$
$$CO + H_2O \leftrightarrow H_2 + CO_2 \qquad (8)$$
$$C + CO_2 \leftrightarrow 2CO \qquad (9)$$
$$2CO + 2H_2 \leftrightarrow CH_4 + CO_2 \qquad (10)$$
$$C + 2H_2 \leftrightarrow CH_4 \qquad (11)$$

According to Encinar et al. [14], the steam gasification reaction (7) and the water gas shift reaction (8) are dominant under atmospheric pressure at 600-800ºC, while the reaction (9) tends to occur at high temperature and the reactions (10) and (11) occur under the condition of high pressure. However, the steam gasification in this

study was carried out under atmospheric pressure at 700-800ºC and the CH_4 was hardly produced, indicating that the main reactions are (7) and (8). Furthermore, it can be seen that the reaction of (8) is easy to occur in HOFA-2 and HOFA-3 because the amount of CO_2 evolution was larger than that of CO evolution. Therefore, the increase of ash content in HOFA promotes the water gas shift reaction by steam gasification.

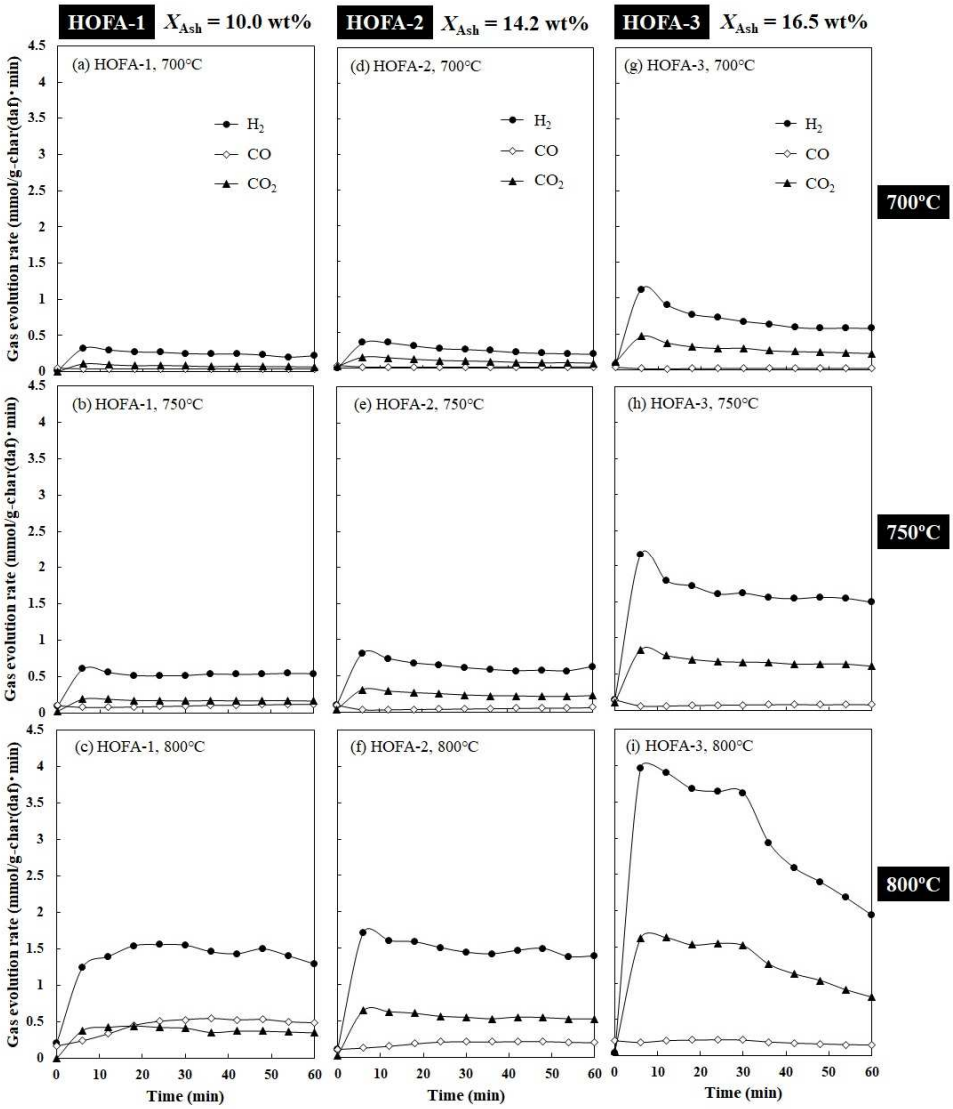

Fig. 4. Gas evolution profiles for HOFA during steam gasification at 700, 750, 800ºC

Effect of ash in HOFA on steam gasification

In order to investigate the relationship between the ash content and the gaseous evolution, the chemical form of ash in HOFA samples before and after steam gasification at 800ºC was analyzed by XRD, and XRD patterns are shown in Fig.6. In all HOFA samples, α-Fe observed after pyrolysis at 800ºC disappeared after steam gasification for 60 min, and Fe_3O_4 appeared instead. The peak intensity of Fe_3O_4 increased with increasing the amount of iron oxide contained in HOFA. Additionally, the peak of Ni was confirmed even after 60 min of steam gasification, but its peak intensity became smaller than that after pyrolysis. Hence, this indicates that α-Fe and Ni reduced after pyrolysis were oxidized during steam gasification. Here, Fig.7 shows the dependence of the iron oxide and nickel oxide contents in HOFA on the carbon conversion. As the content of iron oxide and nickel oxide increased (HOFA-1 < HOFA-2 < HOFA-3), the carbon conversion also increased. As described above, the amount of H_2

increased with increasing the carbon conversion (Table 5). Therefore, it is also suggested that HOFA, which is rich in iron oxide and nickel oxide, enhance the gasification reaction, and α-Fe and Ni promote the water gas shift reaction (8) rather than the steam gasification reaction of (7).

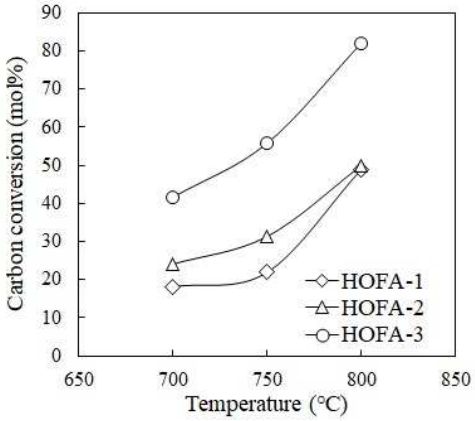

Fig. 5. Relationship between temperature and carbon conversion after gasification of HOFA for 60 min

Table 5. Amount of gas evolution and carbon conversion with HOFA after gasification at 700, 750 and 800ºC for 60 min

Sample		Amount of H_2 evolution mmol/g-char (daf)	Amount of CO evolution mmol/g-char (daf)	Amount of CO_2 evolution mmol/g-char (daf)	Carbon conversion mol%
HOFA-1	700 ºC	14	2.1	4.6	18
	750 ºC	31	6.0	9.9	22
	800 ºC	83	27	22	49
HOFA-2	700 ºC	16	1.1	6.1	24
	750 ºC	37	3.2	14	31
	800 ºC	86	12	32	50
HOFA-3	700 ºC	41	1.1	18	42
	750 ºC	96	4.5	39	56
	800 ºC	179	11	76	82

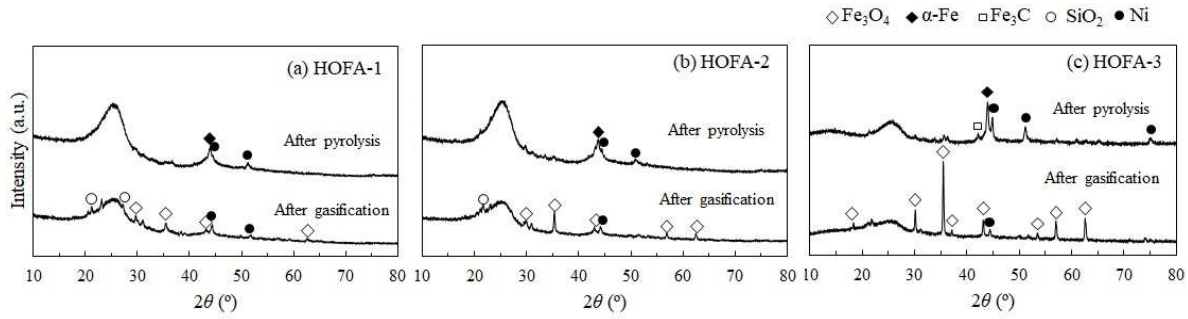

Fig. 6. XRD patterns of HOFA char after pyrolysis and HOFA residue after steam gasification at 800ºC

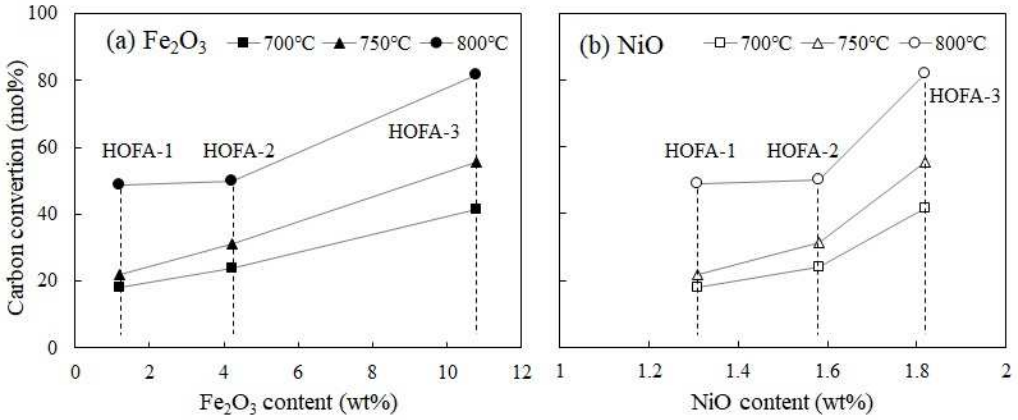

Fig. 7 Dependence of (a) Fe_2O_3 and (b) NiO content on carbon conversion after steam gasification of HOFA-3 for 60 min

Fig.8 shows the relationship between the specific rate and carbon conversion at different temperature. As the carbon conversion increased, the specific rates also increased. This increasing tendency of specific rates appeared remarkably at 800ºC. In particular, the specific rate for HOFA-3 at 800ºC increased dramatically from around 10 mol% of carbon conversion. This indicates that the amount of evolution gas increased even though the carbon content in HOFA char decreased with the progress of steam gasification.

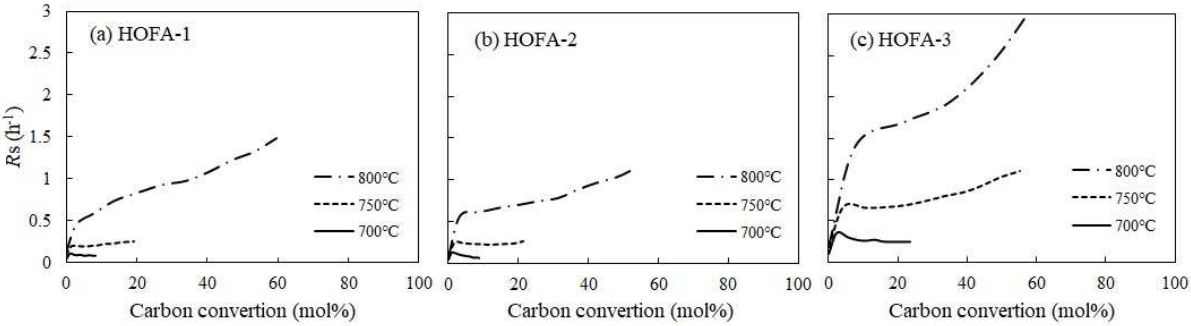

Fig. 8. Profiles for the specific gasification rates of (a) HOFA-1, (b) HOFA-2, (c) HOFA-3 at 700, 750 and 800ºC

In order to investigate the relationship between the chemical form of metal components in HOFA and the rate of gas evolution at the different gasification temperatures, Fig.9 shows the change in XRD patterns of HOFA-3, which has the largest ash content, after steam gasification. The XRD pattern, in which only Fe_3O_4 peak appeared after pyrolysis, did not change during steam gasification at 700ºC. While α-Fe and Fe_3C were observed after pyrolysis at 750ºC, these peaks disappeared with progress of steam gasification and Fe_3O_4 was observed instead. Also, Ni peak appeared after steam gasification for 12 min. After pyrolysis at 800ºC, sharp peaks of α-Fe, Fe_3C and Ni were observed, but Fe_3O_4 appeared after 6 min. Although the peak intensity of Ni became small slightly, Ni in HOFA remained even after steam gasification for 60 min. It is already known that H_2 evolution during steam gasification of lignite was promoted by the presence of α-Fe [17,18], and the water-gas shift reaction with Ni-based catalysts was enhanced by suppressing tar cracking [19-22]. Therefore, it is considered that the metal catalyst such as α-Fe and Ni has effectiveness for improving the gasification reaction. As shown in Fig.9, the Fe and Ni species were not reduced to α-Fe and Ni at 700ºC, so that the gasification reaction hardly proceeded (Fig.8). On the other hand, at 750ºC and 800ºC, the gasification reaction is rapidly accelerated because α-Fe produced after pyrolysis is present in HOFA. Furthermore, since Ni keeps to exist in HOFA during steam gasification, the gasification reaction promoted even if the carbon content decreased.

The activation energy, which was calculated at a carbon conversion of 5 mol%, for HOFA-1, HOFA-2 and HOFA-3 was 168, 163 and 113 kJ/mol, respectively, and the activation energy for HOFA-3 was the lowest. From this result, it is suggested that the reactivity of HOFA-3 was the highest. Hence, the reduced α-Fe and Ni maintained the catalytic activity for 60 min of steam gasification and promoted the reaction between steam and carbon in HOFA.

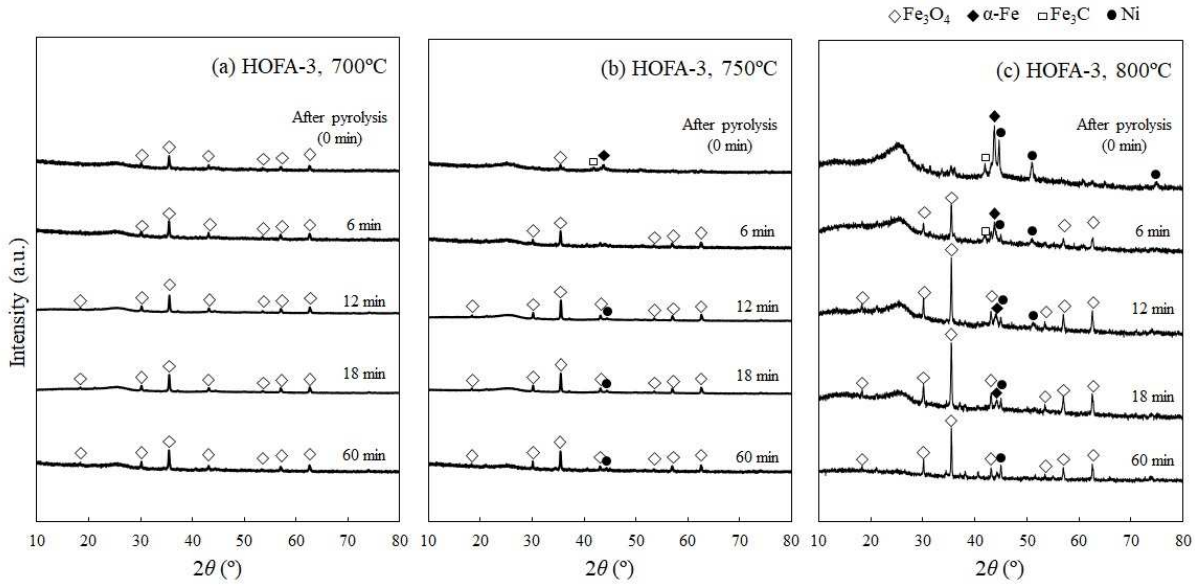

Fig. 9. XRD patterns residue for HOFA-3 after steam gasification at (a)700, (b)750, (c)800°C

To examine whether α-Fe and Ni in HOFA is effective as a catalyst during the gasification reaction, the steam gasification was performed using demineralized HOFA, i.e. DHOFA-1, DHOFA-2 and DHOFA-3. The color of filtrate after demineralization was turned yellow-green, and the peak of Fe_3O_4 disappeared from the XRD pattern shown in Fig.10, indicating that iron oxide and nickel oxides were removed from HOFA. In addition, the ash content of DHOFA-1, DHOFA-2 and DHOFA-3 are 4.6, 5.2 and 3.6 wt%, which are similar to the sum of the contents of SiO_2 and Al_2O_3 (3-5 wt%). After pyrolysis at 800ºC, the char yield of DHOFA-1, DHOFA-2 and DHOFA-3 were 93, 89 and 91 wt%. The volatile matter decreased by elution of ammonium sulfate in water, so that the char yields before and after demineralization were very different. From the XRD patterns as shown in Fig.10, it was found that not only the peak of Fe_3O_4 but also the peak of ammonium sulfate disappeared after demineralization. Also, Table 6 shows the amount of evolution gas and the carbon conversion for demineralized HOFA at 800ºC. Compared to the results for HOFA without demineralization treatment (Table 5), the amount of evolution gas and the carbon conversion were significantly decreased. Furthermore, the water-gas shift reaction was suppressed because the amount of CO evolution increased, while the amount of CO_2 evolution tended to decreased. It is presumed that the steam gasification using DHOFA is difficult to occur at 800ºC due to lack of the heavy metal component for working as a catalyst. In conclusion, the reduced heavy metal components such as α-Fe and Ni affect the evolution of flammable gas during steam gasification, suggesting that HOFA containing a large amount of iron oxide and nickel oxide is suitable to generate in the evolution of flammable gas.

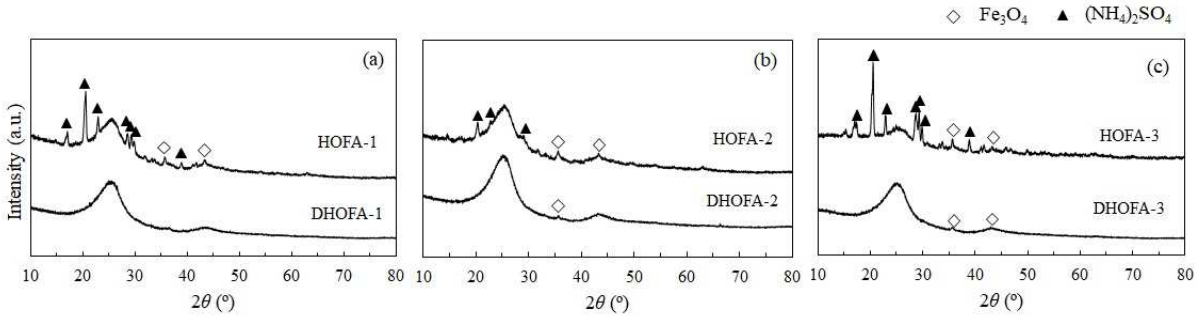

Fig. 10. XRD patterns for (a) HOFA-1, (b) HOFA-2, (c) HOFA-3 before and after decalcification

Table 6. Amount of gas evolution and carbon conversion for DHOFA after steam gasification at 800°C for 60 min

Sample	Amount of H_2 evolution mmol/g-char(daf)	Amount of CO evolution mmol/g-char(daf)	Amount of CO_2 evolution mmol/g-char(daf)	Carbon conversion mol%
DHOFA-1	25	10	5.3	14
DHOFA-2	16	6.1	3.3	13
DHOFA-3	22	7.7	5.1	13

CONCLUSION

In order to utilize HOFA effectively, the steam gasification of HOFA at 700-800ºC was performed, and the effect of heavy metal components in HOFA on the amount of gas evolution was investigated. H_2, CO and CO_2 gases were generated by steam gasification of HOFA, so that the amount of H_2 evolution was the largest among the evolution gases. As the gasification temperature and the amount of ash content in HOFA increased, the water gas shift reaction was promoted, and the amount H_2 evolution increased. XRD analysis of HOFA before and after gasification was carried out to consider the effective metal species for gasification reaction. It was found that iron oxide and nickel oxide remained in HOFA after HOFA was pyrolyzed at 700ºC, but these oxides were reduced to α-Fe and Ni by pyrolysis at 750ºC and 800ºC. The α-Fe was oxidized with progressing gasification, and Ni existed in the HOFA even after steam gasification for 60 min. Also, the amount of H_2 evolution increases with increasing Fe and Ni contents in HOFA, suggesting that Fe and Ni species have an effect as a catalyst for promoting the gasification reaction.

ACKNOWLEDGEMENTS

The authors thank the Sumitomo Foundation in Japan (No.193156) for the financial support. Parts of measurement were supported in Akita Industrial Technology center.

REFERENCES

1. K. Murakami, T. Kato, and K. Sugawara, “Combustion characteristics of mixtures of heavy oil ash and waste plastic”, Journal of the Japan Institute of Energy, Vol. 89, No. 10, pp. 1006-1011, 2010.
2. S. Vitolo, M. Seggiani, S. Filippi, and C. Brocchini, “Recovery of vanadium from heavy oil and Orimulsion fly ashes”, Hydrometallurgy, Vol. 57, No. 2, pp. 141-149, 2000.
3. M. A. Al-Ghouti, Y. S. Al-Degs, A. Gjrair, H. Khoury, and M. Ziedan, “Extraction and separation of vanadium and nickel from fly ash produced in heavy fuel power plants”, Chemical Engineering Journal, Vol. 173, No. 1, pp. 191-197, 2011.
4. Y. S. Al-Degs, A. Ghrir, H. Khoury, G. M. Walker, M. Sunjuk, and M. A. Al-Ghouti, “Characterization and utilization of fly ash of heavy fuel oil generated in power stations”, Fuel Processing Technology, Vol. 123, pp. 41-46, 2014.
5. M. Seggiani, G. Teti, and S. Vitolo, “Investigation on the combustion of heavy-oil fly-ashes”, Fuel, Vol. 81, No. 13, pp. 1711-1715, 2002.

6. X. Li, W. Miao, Y. Lv, Y. Wang, C. Gao, and D. Jiang, "TGA-FTIR investigation on the co-combustion characteristics of heavy oil fly ash and municipal sewage sludge", Thermochimica Acta, Vol. 666, pp. 1-9, 2018.
7. T. Popa, M. Fan, M. D. Argyle, M. D. Dyar, Y. Gao, J. Tang, E. A. Speicher, D. M. Kammen, "H_2 and CO_x generation from coal gasification catalyzed by a cost-effective iron catalyst", Applied Catalysis A: General, Vol. 464-465, pp. 207-217, 2013.
8. X. Li, H. Wu, J. Hayashi, and C.-Z. Li, "Volatilization and catalytic effects of alkali and alkaline earth metallic species during the pyrolysis and gasification of Victorian brown coal. Part VI. Further investigation into the effects of volatile-char interactions", Fuel, Vol. 83, No. 10, pp. 1273-1279, 2004.
9. K. Murakami, M. Sato, N. Tsubouchi, Y. Ohtsuka, and K. Sugawara, "Steam gasification of Indonesian subbituminous coal with calcium carbonate as a catalyst raw material", Fuel Processing Technology, Vol. 129, pp. 91-97, 2015.
10. K. Śpiewak, G. Czerski, and S. Porada, "Effect of K, Na and Ca-based catalysts on the steam gasification reactions of coal. Part I: Type and amount of one-component catalysts", Chemical Engineering Science, Vol. 229, No. 16, pp. 116024, 2020.
11. Z. Yang, J. Hu, Y. Li, Y. Chen, K. Qian, H. Yang, and H. Chen, "Catalytic steam gasification of Mengdong coal in the presence of iron ore for hydrogen-rich gas production", Journal of the Energy Institute, Vol. 92, No. 2, pp. 391-402, 2019.
12. L. Shen, and K. Murakami, "Steam co-gasification of iron-loaded biochar and low-rank coal", International Journal of Energy Research, Vol. 40, No. 13, pp. 1846-1854, 2016.
13. JIS M8812 2004 Coal and Coke–Methods for proximate analysis, https://kikakurui.com/m/M8812-2006-01.html.
14. J. M. Encinar, J. F. Gonzláez, and J. Gonzláez, "Steam gasification of Cynara cardunculus L.: influence of variables", Fuel Processing Technology, Vol. 75, No. 1, pp. 27-43, 2002.
15. J. Wang, M. Jian, Y. Yao, Y. Zhang, and J. Cao, "Steam gasification of coal char catalyzed by K_2CO_3 for enhanced production of hydrogen without formation of methane", Fuel, Vol. 88, No. 9, pp. 1572-1579, 2009.
16. S. Porada, G. Czerski, T. Dziok, P. Grzywacz, and D. Makowska, "Kinetics of steam gasification of bituminous coals in terms of their use for underground coal gasification", Fuel Processing Technology, Vol. 130, pp. 282-291, 2015.
17. J. Yu, F.-J. Tian, M. C. Chow, L. J. McKenzie, and C.-Z. Li, "Effect of iron on the gasification of Victorian brown coal with steam: enhancement of hydrogen production", Fuel, Vol. 85, No. 2, pp. 127-133, 2006.
18. Y. Jiang, H. Yan, Q. Guo, F. Wang, and J. Wang, "Multiple synergistic effects exerted by coexisting sodium and iron on catalytic steam gasification of coal char", Fuel Processing Technology, Vol. 191, pp. 1-10, 2019.
19. L. Li, K. Morishita, H. Mogi, K. Yamasaki, and T. Takarada, "Low-temperature gasification of a woody biomass under a nickel-loaded brown coal char", Fuel Processing Technology, Vol. 91, No. 8, pp. 889-894, 2010.
20. A. Tomita, Y. Ohtsuka, and Y. Tamai, "Low temperature gasification of brown coals catalyzed by nickel", Fuel, Vol. 62, No. 2, pp. 150-154, 1983.
21. A. Tomita, Y. Watanabe, T. Takarada, Y. Ohtsuka, and Y. Tamai, "Nickel-catalysed gasification of brown coal in a fluidized bed reactor at atmospheric pressure", Fuel, Vol. 64, No. 6, pp. 795-800, 1985.
22. C. Phuhiran, T. Takarada, and S. Chaiklangmuang, "Hydrogen-rich gas from catalytic steam gasification of eucalyptus using nickel-loaded Thai brown coal char catalyst", International Journal of Hydrogen Energy, Vol. 39, No. 8, pp. 3649-3656, 2014.